Development 138, 4334 (2011) doi:10.1242/dev.073650

Cell cycle arrest in node cells governs ciliogenesis at the node to break left-right symmetry

Yoshihiro Komatsu, Vesa Kaartinen and Yuji Mishina

There was an error published in the ePress version of *Development* **138**, 3915-3920 published on 10 August 2011.

On p. 3919, in the legend for Fig. 4, asymmetry was incorrectly referred to as symmetry. The correct sentence appears in full below:

Subsequently, nodal cilia develop and nodal flow is generated, which triggers the establishment of left-right asymmetry.

The replacement ePress article published on 17 August 2011, the online issue and print copy are correct.

We apologise to authors and readers for this error.

Development 138, 3915-3920 (2011) doi:10.1242/dev.068833

Cell cycle arrest in node cells governs ciliogenesis at the node to break left-right symmetry

Yoshihiro Komatsu, Vesa Kaartinen and Yuji Mishina*

SUMMARY

Cilia at the node generate a leftward fluid flow that breaks left-right symmetry. However, the molecular mechanisms that regulate ciliogenesis at the node are largely unknown. Here, we show that the epiblast-specific deletion of the gene encoding the BMP type 1 receptor (*Acvr1*) compromised development of nodal cilia, which results in defects in leftward fluid flow and, thus, abnormalities in left-right patterning. *Acvr1* deficiency in mouse embryonic fibroblasts (MEFs) resulted in severe defects in their quiescence-induced primary cilia. Although the induction of quiescence in wild-type MEFs leads to an increase in the level of the cyclin-dependent kinase inhibitor $p27^{Kip1}$ and to rapid $p27^{Kip1}$ phosphorylation on Ser^{10}, MEFs deficient in *Acvr1* show a reduction in both $p27^{Kip1}$ protein levels and in $p27^{Kip1}$ Ser^{10} phosphorylation. The observed defects in cilium development were rescued by the introduction of $p27^{Kip1}$ into *Acvr1*-deficient MEFs, implying that BMP signaling positively controls $p27^{Kip1}$ stability in the G0 phase via $p27^{Kip1}$ Ser^{10} phosphorylation, which is a prerequisite for induction of primary cilia. Importantly, in control embryos, $p27^{Kip1}$ protein is clearly present and strongly phosphorylated on Ser^{10} in cells on the quiescent ventral surface of the node. By contrast, the corresponding cells in the node of *Acvr1* mutant embryos were proliferative and showed a dramatic attenuation in both $p27^{Kip1}$ protein levels and phosphorylation on Ser^{10}. Our data suggest that cell quiescence controlled by BMP signaling via ACVR1 is required for transient formation of nodal cilia, and provide insight into the fundamental question of how the node represents the mechanistic 'node' that regulates the development of left-right symmetry in vertebrates.

KEY WORDS: BMP signaling, Cell cycle, Cilia, Left-right determination, Node

INTRODUCTION

The node in mammals is structurally and functionally homologous to Kupffer's vesicle in zebrafish, Spemann's organizer in amphibia and Hensen's node in chick (Hamada et al., 2002; Hirokawa et al., 2006; Levin, 2005; Sulik et al., 1994; Tabin, 2006). This transient embryonic structure has the ability to induce the axial specification during establishment of the embryonic body plan (Tam and Behringer, 1997). In the mouse embryo, the fully formed node is located at the anterior end of the primitive streak (Lee and Anderson, 2008). It has dorsal and ventral surfaces, and contains 200 to 300 ciliated cells (Hamada et al., 2002; Sulik et al., 1994). Recent studies have shown that nodal cilia are functional and that their rotational movement generates a leftward fluid flow (nodal flow), breaking the left-right symmetry in mouse embryos (Becker-Heck et al., 2011; Blum et al., 2007; Hirokawa et al., 2006; Nonaka et al., 1998). Despite the importance of cilia at the node, very little is known about the fundamental mechanisms that regulate ciliogenesis at the node in vivo.

Bone morphogenetic proteins (BMPs) play an essential role in establishment of the left-right patterning in vertebrates (Fujiwara et al., 2002; Furtado et al., 2008; Mine et al., 2008; Ramsdell and Yost, 1999; Yokouchi et al., 1999). We have previously reported that one of the BMP type I receptors, *Acvr1*, is required for the left-right patterning in the mouse (Kishigami et al., 2004). However, molecular details underlying the role of BMP signaling in this process are still unclear. In this paper, we took advantage of a conditional gene knockout approach to assess the requirement of BMP signaling during establishment of left-right asymmetry. We found that BMP signaling through a type 1 receptor (ACVR1) is important for formation of nodal cilia. BMP signaling positively controls the phosphorylation of a cyclin-dependent kinase inhibitor $p27^{Kip1}$ (Cdkn1b – Mouse Genome Informatics), which maintains cells in quiescence, a crucial process for the induction of primary cilia. Notably, both $p27^{Kip1}$ and phospho-$p27^{Kip1}$ are produced exclusively at the node under the tight regulation of BMP signaling when embryos start to break left-right symmetry. Our results suggest that BMP signaling is essential for inducing cell cycle arrest at the node and for triggering development of nodal cilia.

MATERIALS AND METHODS

Animal and genotyping analysis

Generation of *Acvr1* heterozygous mice, *Acvr1* floxed mice, *Mox2-Cre* mice and ROSA26 reporter mice have been reported previously (Kaartinen and Nagy, 2001; Komatsu et al., 2007; Mishina et al., 1999; Soriano, 1999; Tallquist and Soriano, 2000). All mouse experiments were performed in accordance with University of Michigan's guidelines covering the humane care and use of animals in research.

In situ hybridization and immunohistochemistry

In situ hybridization was performed using standard procedures (Komatsu et al., 2007). Immunohistochemistry was performed as described previously (Bellomo et al., 1996). Antibodies used in this study were against: acetylated tubulin (Sigma, T6793), γ-tubulin (Sigma, T5326), γ-tubulin (Sigma, T6557), Ki-67 (Dako, M7249), p27 (BD Transduction Laboratories, 610241), p27 phospho Ser10 (Abcam, ab62364), p21 (BD Transduction Laboratories, 556431), p57 (Santa Cruz, sc-1039), retinoblastoma (BD Pharmingen, 554136), cyclin D1 (Santa Cruz, sc-8396), phospho SMAD1/5/8 (Cell Signaling, 9511) and β-Actin (Sigma, A5441).

Department of Biologic and Materials Sciences, School of Dentistry, University of Michigan, 1011 North University Avenue, Ann Arbor, MI 48109-1078, USA.

*Author for correspondence (mishina@umich.edu)

Accepted 4 July 2011

Scanning electron microscopy

Embryos were fixed with 2% paraformaldehyde and 2.5% glutaraldehyde. Following postfixation in 1% buffered osmium tetroxide, the samples were dehydrated with ethanol and critical point-dried using carbon dioxide as the transition solvent. Embryos were mounted on aluminum stubs with silver paste and sputter-coated with a 20 nm thickness of gold:palladium alloy 60:40. Samples were examined with a JEOL scanning electron microscope using an acceleration voltage of 20 kV. Cilia length was measured by ImageJ software.

Observation of the nodal flow

Nodal flow observation was performed as described previously (Nonaka et al., 1998). Beads movements were observed with an Olympus BX-51 microscope by Olympus PlanApo 60×/1.40 objective lens. Images were captured with a CCD camera (KP-M1U, Hitachi Denshi), converted (ADVC-300, Canopus Co.) and recorded. Embryos were genotyped by PCR after nodal flow observation.

Generation of mouse embryonic fibroblast (MEF) and adenovirus transduction

Acvr1$^{flox/flox}$ carried with ROSA26 reporter MEF were established from E12.5 embryos. MEF were grown in DMEM with 10% fetal bovine serum (Hyclone). Adenovirus (Ad)-*lacZ*, Ad-GFP, Ad-Cre (Vector Development Laboratory, Baylor College of Medicine) and Ad-p27^{Kip1} (Vector Biolabs) were used. After transduction of Ad-*lacZ* or Ad-Cre, MEF were stained with fluorescein di-β-galactoside (Invitrogen) and sorted by flow cytometry.

Immunoblot analysis

MEF extracts were prepared using RIPA buffer. Cell lysates were applied for SDS-PAGE and transferred to Amersham Hybond-P membrane. Signal was detected using ECL western blotting reagents (GE Healthcare).

RESULTS AND DISCUSSION

We disrupted *Acvr1* in an epiblast-specific manner by using the *Mox2-Cre* driver line (Kaartinen and Nagy, 2001; Komatsu et al., 2007; Mishina et al., 1999; Tallquist and Soriano, 2000) (see Fig. S1 in the supplementary material) (*Acvr1* cKO hereafter). Unlike conventional *Acvr1* knockout embryos (Mishina et al., 1999), *Acvr1* cKO embryos developed beyond gastrulation and died around embryonic day 11.5 (E11.5). *Acvr1* cKO embryos displayed altered head structures, and abnormal embryonic turning, heart looping and limb bud development (Fig. 1A; see Fig. S2 in the supplementary material); these features are frequently observed in mice displaying defects in left-right patterning. Therefore, we first examined expression of the left side-specific genes *Nodal* (Collignon et al., 1996; Lowe et al., 1996), *Lefty2* (Meno et al., 1996) and *Pitx2* (Yoshioka et al., 1998) (Fig. 1B). In *Acvr1* cKO embryos, expression of *Nodal*, *Lefty2* and *Pitx2* in the lateral plate mesoderm was either left-sided (≈40%) or bilateral (≈60%). We also analyzed the midline marker *Lefty1*, which is required for attenuation of the left side-specific genes on the right side of the embryo (Meno et al., 1998). Although the floor plate markers *Shh* and *Foxa2* were expressed normally (Echelard et al., 1993; Sasaki and Hogan, 1993), *Lefty1* expression was downregulated in *Acvr1* cKO embryos (Fig. 1B). These results confirm that *Acvr1* is required for correct left-right patterning during early mouse development.

To assess whether *Acvr1* has a primary role in the establishment of left-right asymmetry, we investigated structural features of the node at E7.75 to E8.0 using scanning electron microscopy. When viewed from the ventral side, wild-type embryos showed a cup-shaped node with evenly distributed ciliated cells; the *Acvr1* cKO embryos displayed morphological changes at the node that were characterized by a flat shape, the presence of atypical bulging cells (Fig. 2A) and notably shortened cilia (Fig. 2B). These data indicate that although the node was formed in the mutant embryos, the formation of nodal cilia was compromised. Because the shortened cilia may lead to abnormal nodal flow (Beckers et al., 2007), we examined whether nodal flow was altered in *Acvr1* cKO embryos. The majority of *Acvr1* cKO embryos (13/16) showed random and Brownian motion movement of the beads, which required more time to reach to the left edge of the node compared with that of wild-type embryos (Fig. 2C; see Movies 1 and 2 in the supplementary material). These results indicate that BMP signaling through ACVR1 is required for appropriate formation of nodal cilia.

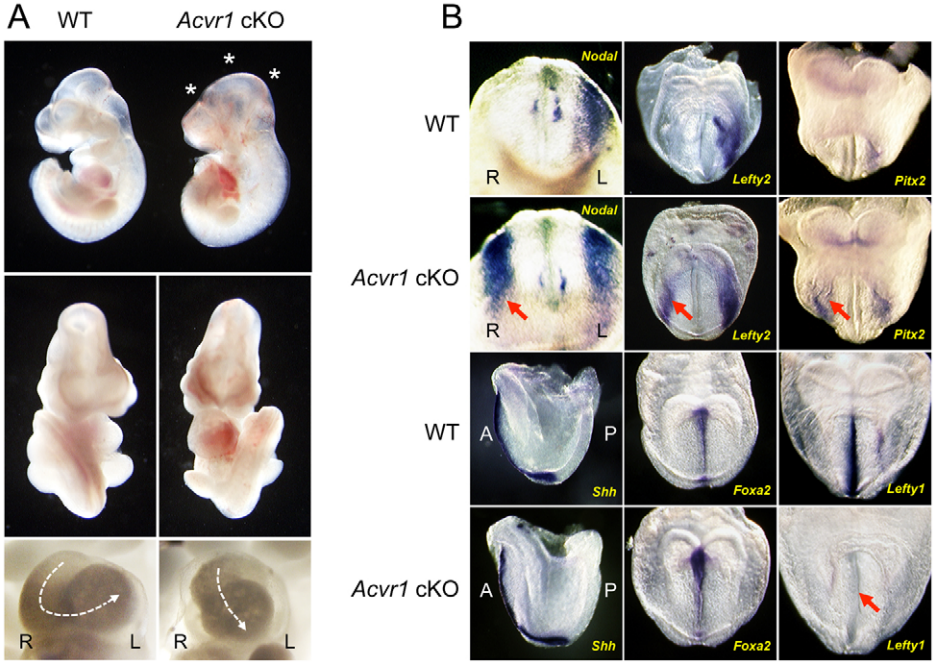

Fig. 1. BMP signaling through ACVR1 regulates left-right patterning. (**A**) Whole-mount view of wild-type and *Acvr1* cKO embryos at E10.5. *Acvr1* cKO embryos showed abnormalities in head (white asterisks, top panel), embryonic turning (middle panel) and cardiac looping (bottom panel). (**B**) Expression patterns of *Nodal*, *Lefty2*, *Pitx2*, *Shh*, *Foxa2* and *Lefty1* are shown. Ventral view for *Nodal*. Frontal view for *Lefty2*, *Pitx2*, *Foxa2* and *Lefty1*. Lateral view for *Shh*. Red arrows show aberrant right-sided expression of *Nodal*, *Lefty2* and *Pitx2* (second panel from the top), and absent midline expression of *Lefty1* (bottom panel) in *Acvr1* cKO mutants. A, anterior; P, posterior; L, left; R, right.

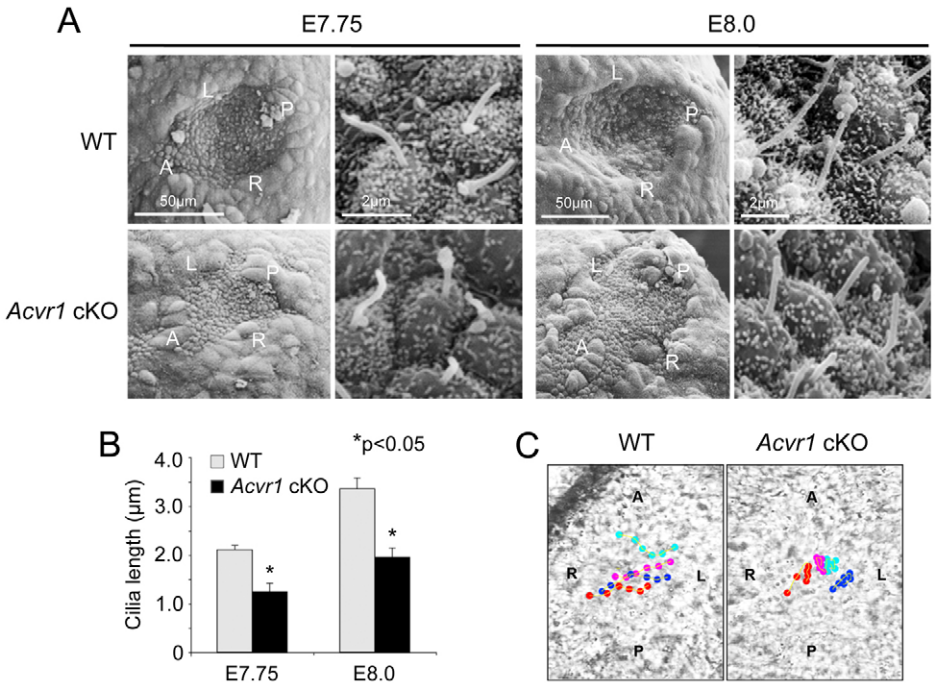

Fig. 2. Structural abnormalities at node and alteration of the nodal flow. (**A**) Scanning electron microscopic analysis of the node at E7.75 and E8.0. Low- and high-magnification images are shown. (**B**) Nodal cilia were significantly shorter in *Acvr1* cKO embryos at E7.75 and E8.0. Four embryos for each stage were analyzed and more than 50 nodal cilia per embryo were measured. Data are mean+s.e.m. (**C**) Examples of the movement of beads in the node. The movements of four individual beads represented by different colors were traced on videograms. Bead migration from the right edge to the left edge of the node within 10 seconds was regarded as a consistent leftward flow. Movements of at least four beads per embryo were monitored to judge the presence of the leftward flow in a given embryo. A, anterior; P, posterior; L, left; R, right.

Although the molecular mechanisms that initiate formation of transient nodal cilia are largely unknown, it has been reported that node cells are quiescent in mouse embryos at E7.75-E8.2 (Bellomo et al., 1996), the crucial period when the formation of nodal cilia is initiated. In addition, it has been shown that cells need to be quiescent in order to develop primary cilia in tissue culture (Tucker et al., 1979). Together with our previous discovery that *Acvr1* is expressed in ventral surface of the node (Kishigami et al., 2004), these observations prompted us to test the hypothesis that the primary role of BMP signaling through ACVR1 is to induce cellular quiescence, thus allowing node cells to develop cilia. To address the role of ACVR1 in regulation of cell cycle and cilia development, we generated *Acvr1*-deficient mouse embryonic fibroblasts (MEFs) (see Fig. S3 in the supplementary material). When cultured to the high cell density, 60% of control MEFs (Ad-*lacZ*), but only about 20% of *Acvr1*-deficient MEFs (Ad-Cre), developed primary cilia (Fig. 3A,B). We also analyzed the cells for the presence of Ki-67, which marks actively dividing cells (Starborg et al., 1996). Fewer than 20% of control MEFs, but still more than 50% of *Acvr1*-deficient MEFs stained positive for Ki-67 (Fig. 3A,B). Both control and *Acvr1*-deficient MEF cells grew normally (see Fig. S4 in the supplementary material). These results reveal that BMP signaling through ACVR1 is required for induction of the quiescence, a prerequisite for developing primary cilia (Tucker et al., 1979). Cell cycle arrest in MEFs can be induced by the Cip/Kip family of cyclin-dependent kinase inhibitors, including $p27^{Kip1}$ (Toyoshima and Hunter, 1994). It also has been suggested that phosphorylation of $p27^{Kip1}$ on Ser^{10} is required to stabilize $p27^{Kip1}$ protein during the quiescent phase (Kotake et al., 2005). Thus, we investigated $p27^{Kip1}$ protein levels and levels of $p27^{Kip1}$ phosphorylation on Ser^{10} in control and *Acvr1*-deficient MEFs. During primary cilia induction, both $p27^{Kip1}$ protein levels and phosphorylation on Ser^{10} were increased in control MEFs (Fig. 3C). However, in *Acvr1*-deficient MEFs, the level of $p27^{Kip1}$ protein was decreased (Fig. 3C; see Fig. S5 in the supplementary material) and $p27^{Kip1}$ phosphorylation on Ser^{10} was attenuated (Fig. 3C). The retinoblastoma (Rb) and cyclin D1 protein levels were comparable in control and *Acvr1*-deficient MEFs (Fig. 3C), showing initial cell cycle progression occurred normally in both MEFs. In addition, we observed that formation of primary cilia was restored by introduction of $p27^{Kip1}$ using adenoviral gene transfer (Ad-p27) into *Acvr1*-deficient MEFs (Fig. 3D,E). These data suggest that BMP signaling through ACVR1 positively regulates the stabilization of $p27^{Kip1}$ to keep MEFs in the quiescent phase to allow formation of primary cilia.

Next, we analyzed expression of $p27^{Kip1}$ at the node of mouse embryos. Importantly, all the cells on ventral surface of the node stained positive for $p27^{Kip1}$ and for $p27^{Kip1}$ phospho-Ser^{10} (Fig. 4A; see Fig. S6 in the supplementary material), supporting the idea that stabilization of $p27^{Kip1}$ via phosphorylation on Ser^{10} at the node is required for quiescence and for subsequent formation of nodal cilia. In agreement with this, Ki-67 was undetectable in $p27^{Kip1}$-positive cells (Fig. 4A; see Fig. S6 in the supplementary material). By contrast, both $p27^{Kip1}$ protein levels and $p27^{Kip1}$ phosphorylation levels on Ser^{10} were significantly reduced in cells on ventral surface of the node in *Acvr1* cKO embryos (Fig. 4A). Consistent with the results from *Acvr1*-deficient MEFs (Fig. 3), the cells on the ventral surface of node in *Acvr1* cKO embryos were

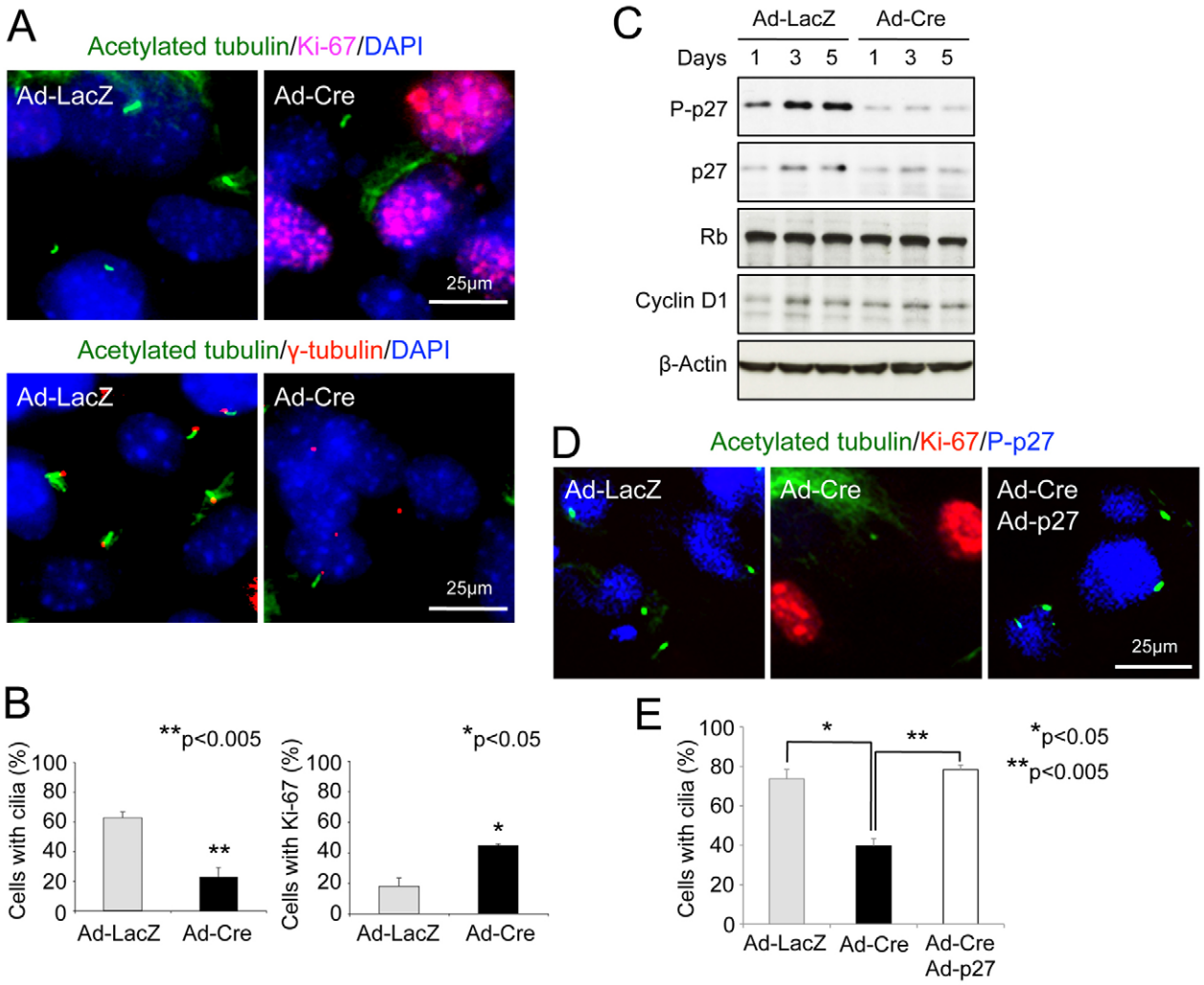

Fig. 3. BMP signaling through ACVR1 is required for the primary cilia formation via the regulation of $p27^{Kip1}$. (**A**) A significant reduction in the number of primary cilia (green, acetylated tubulin) and increased levels of a cell proliferation marker (red, Ki-67) were observed in *Acvr1*-deficient MEFs (upper panels), whereas γ-tubulin (red) was seen in both control and mutant MEFs (lower panels). (**B**) Differences in the number of cilia and in cell proliferation rates between control MEFs (Ad-*lacZ* transduced cells, gray) and *Acvr1*-deficient MEFs (Ad-Cre transduced cells, black). More than 100 cells were randomly analyzed in three independent experiments. Data are mean+s.e.m. (**C**) Cell lysates were prepared at days 1, 3 and 5 during cilia formation and cell cycle regulators were analyzed by western blotting. (**D**) Defective formation of the primary cilia (green, acetylated tubulin) in *Acvr1*-deficient MEFs (middle) coincided with the increased levels of a cell proliferation marker (red, Ki-67) and attenuated phosphorylation of $p27^{Kip1}$ on Ser^{10} (blue, phospho-Ser^{10} in $p27^{Kip1}$). Cilia formation was restored with adenoviral transduction of $p27^{Kip1}$ (Ad-p27) into *Acvr1*-deficient MEFs (right). (**E**) Differences in a number of cilia from D in three independent experiments. Data are mean+s.e.m.

proliferative, as demonstrated by positive Ki-67 staining (Fig. 4A). A role in the regulation of quiescence at the node seems to be specific for $p27^{Kip1}$, as the other members of the Cip/Kip family of Cdk inhibitors ($p21^{Cip1}$ and $p57^{Kip2}$) were not produced at the node (see Fig. S7 in the supplementary material). These data demonstrate that BMP signaling via ACVR1 is required at the node for the induction of quiescence by stabilizing the $p27^{Kip1}$ protein, which is prerequisite for development of the nodal cilia. As a result, the nodal flow is generated that, in turn, triggers the breaking of left-right symmetry (Fig. 4B).

Primary cilia are regarded as postmitotic structures of quiescent cells (Santos and Reiter, 2008). Ciliary dynamics thus appears to be precisely coordinated with a cell cycle progression, but the molecular cues that trigger ciliogenesis at the node are poorly understood. Our results demonstrate that BMP signaling through ACVR1 controls the stability of $p27^{Kip1}$ via $p27^{Kip1}$ phosphorylation on Ser^{10} to induce the cell quiescence that leads to the formation of nodal cilia. Although mutant mice lacking either $p27^{Kip1}$ or $p27^{Kip1}$ phospho-Ser^{10} are viable (Chu et al., 2008), the situs of the visceral organs and ciliogenesis, including nodal cilia, in these mutants have not been examined. Importantly, several mouse models of polycystic kidney disease generated by mutating ciliogenic genes show downregulation of $p27^{Kip1}$ (Alcalay et al., 2008; Cadieux et al., 2008). Thus, it will be interesting to determine whether dysregulation of cell cycle via $p27^{Kip1}$ causes primary ciliary dyskinesia and situs inversus.

Breaking of left-right symmetry is dependent on nodal cilia-generated leftward fluid flow at the node (Hamada et al., 2002; Hirokawa et al., 2006; Nonaka et al., 1998). But why nodal cilia are formed exclusively at the node during a limited time window

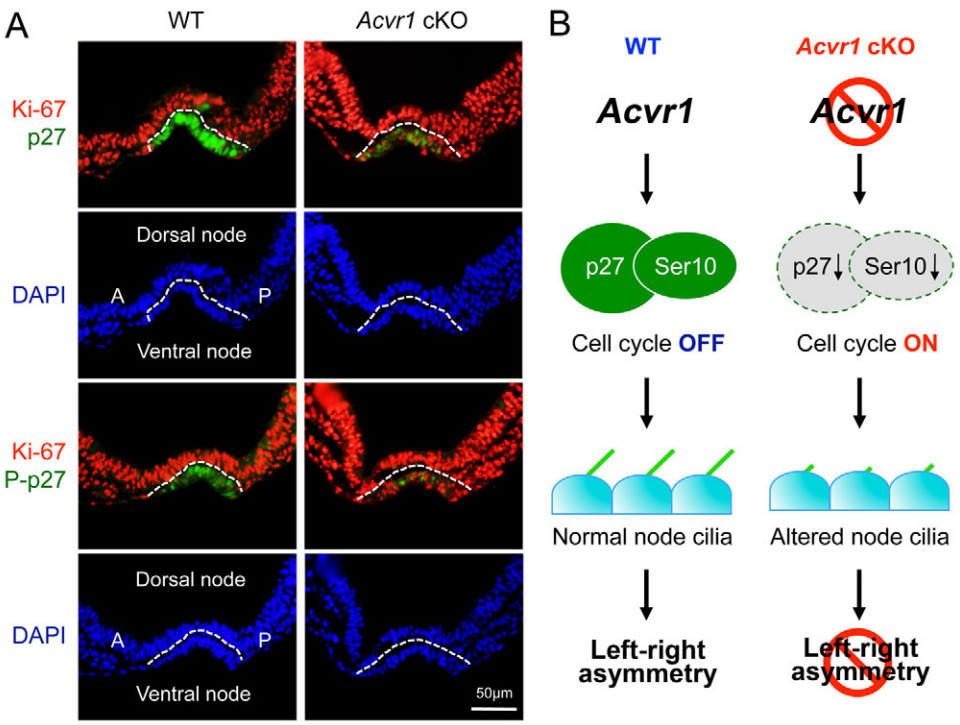

Fig. 4. Cell cycle arrest regulated by BMP signaling is crucial for the transient nodal cilia formation. (**A**) Levels of both $p27^{Kip1}$ and $p27^{Kip1}$ phosphorylation on Ser^{10} ($P\text{-}p27^{Kip1}$) (green staining) were significantly lower on the ventral surface of the node in *Acvr1* cKO embryos at E7.75. In wild-type embryos, cells on ventral surface of the node were quiescent (no detectable Ki-67 staining), whereas corresponding cells in *Acvr1* cKO embryos were proliferative (stained positive for Ki-67). A, anterior; P, posterior. (**B**) A mechanism by which BMP signaling through ACVR1 regulates development of nodal cilia in mouse embryo. The presence of ACVR1 leads to a stabilization of $p27^{Kip1}$ via phosphorylation on Ser^{10}, thus inducing quiescence. Subsequently, nodal cilia develop and nodal flow is generated, which triggers the establishment of left-right asymmetry. If *Acvr1* is deleted, phosphorylation on Ser^{10} is attenuated, leading to a destabilization of $p27^{Kip1}$ at the node. As a result, nodal cilia are not developed appropriately, which leads to a failure of nodal flow and to a failure to break left-right symmetry.

has been an unresolved issue ever since. Our study provides novel insight into a mechanism by which growth factor signaling governs ciliogenesis at the node, which is crucial for the establishment of left-right asymmetry.

Acknowledgements

We thank Dr Shigenori Nonaka for advice about nodal flow experiments; Drs Penny Thomas and Yingzi Yang for suggestions regarding immunohistochemistry; Ms Victoria Madden for scanning electron microscopy; Dr Ajeet Singh for mouse activity; Dr Philippe Soriano for *Mox2-Cre* and ROSA26 reporter mice; Drs Allan Bradley and Robert Crombie for *Acvr1* mice; Drs Hiroshi Hamada, Hiroshi Sasaki, Michael Kuehn, Achim Gossler and Andrew McMahon for in situ probes; Drs Lee Niswander and Jeremy Reiter for fruitful discussion; Drs Penny Thomas, Trisha Castranio and Mitch Eddy for critical reading; and Ms Li He, Chiaki, Nokina and Mirai Komatsu for encouragement. This study is supported by the National Institutes of Health (K99DE021054 to Y.K., R01HL074862 and R01DE013085 to V.K., and R01DE020843 and ES071003-11 to Y.M.) and by a fellowship from the Japan Society for the Promotion of Science (Y.K.). Deposited in PMC for release after 12 months.

Competing interests statement

The authors declare no competing financial interests.

Supplementary material

Supplementary material for this article is available at
http://dev.biologists.org/lookup/suppl/doi:10.1242/dev.068833/-/DC1

References

Alcalay, N. I., Sharma, M., Vassmer, D., Chapman, B., Paul, B., Zhou, J., Brantley, J. G., Wallace, D. P., Maser, R. L. and Vanden Heuvel, G. B. (2008). Acceleration of polycystic kidney disease progression in cpk mice carrying a deletion in the homeodomain protein Cux1. *Am. J. Physiol. Renal Physiol.* **295**, F1725-F1734.

Becker-Heck, A., Zohn, I. E., Okabe, N., Pollock, A., Lenhart, K. B., Sullivan-Brown, J., McSheene, J., Loges, N. T., Olbrich, H., Haeffner, K. et al. (2011). The coiled-coil domain containing protein CCDC40 is essential for motile cilia function and left-right axis formation. *Nat. Genet.* **43**, 79-84.

Beckers, A., Alten, L., Viebahn, C., Andre, P. and Gossler, A. (2007). The mouse homeobox gene Noto regulates node morphogenesis, notochordal ciliogenesis, and left right patterning. *Proc. Natl. Acad. Sci. USA* **104**, 15765-15770.

Bellomo, D., Lander, A., Harragan, I. and Brown, N. A. (1996). Cell proliferation in mammalian gastrulation: the ventral node and notochord are relatively quiescent. *Dev. Dyn.* **205**, 471-485.

Blum, M., Andre, P., Muders, K., Schweickert, A., Fischer, A., Bitzer, E., Bogusch, S., Beyer, T., van Straaten, H. W. and Viebahn, C. (2007). Ciliation and gene expression distinguish between node and posterior notochord in the mammalian embryo. *Differentiation* **75**, 133-146.

Cadieux, C., Harada, R., Paquet, M., Cote, O., Trudel, M., Nepveu, A. and Bouchard, M. (2008). Polycystic kidneys caused by sustained expression of Cux1 isoform p75. *J. Biol. Chem.* **283**, 13817-13824.

Chu, I. M., Hengst, L. and Slingerland, J. M. (2008). The Cdk inhibitor p27 in human cancer: prognostic potential and relevance to anticancer therapy. *Nat. Rev. Cancer* **8**, 253-267.

Collignon, J., Varlet, I. and Robertson, E. J. (1996). Relationship between asymmetric nodal expression and the direction of embryonic turning. *Nature* **381**, 155-158.

Echelard, Y., Epstein, D. J., St-Jacques, B., Shen, L., Mohler, J., McMahon, J. A. and McMahon, A. P. (1993). Sonic hedgehog, a member of a family of putative signaling molecules, is implicated in the regulation of CNS polarity. *Cell* **75**, 1417-1430.

Fujiwara, T., Dehart, D. B., Sulik, K. K. and Hogan, B. L. (2002). Distinct requirements for extra-embryonic and embryonic bone morphogenetic protein 4 in the formation of the node and primitive streak and coordination of left-right asymmetry in the mouse. *Development* **129**, 4685-4696.

Furtado, M. B., Solloway, M. J., Jones, V. J., Costa, M. W., Biben, C., Wolstein, O., Preis, J. I., Sparrow, D. B., Saga, Y., Dunwoodie, S. L. et al. (2008). BMP/SMAD1 signaling sets a threshold for the left/right pathway in lateral plate mesoderm and limits availability of SMAD4. *Genes Dev.* **22**, 3037-3049.
Hamada, H., Meno, C., Watanabe, D. and Saijoh, Y. (2002). Establishment of vertebrate left-right asymmetry. *Nat. Rev. Genet.* **3**, 103-113.
Hirokawa, N., Tanaka, Y., Okada, Y. and Takeda, S. (2006). Nodal flow and the generation of left-right asymmetry. *Cell* **125**, 33-45.
Kaartinen, V. and Nagy, A. (2001). Removal of the floxed neo gene from a conditional knockout allele by the adenoviral Cre recombinase in vivo. *Genesis* **31**, 126-129.
Kishigami, S., Yoshikawa, S., Castranio, T., Okazaki, K., Furuta, Y. and Mishina, Y. (2004). BMP signaling through ACVRI is required for left-right patterning in the early mouse embryo. *Dev. Biol.* **276**, 185-193.
Komatsu, Y., Scott, G., Nagy, A., Kaartinen, V. and Mishina, Y. (2007). BMP type I receptor ALK2 is essential for proper patterning at late gastrulation during mouse embryogenesis. *Dev. Dyn.* **236**, 512-517.
Kotake, Y., Nakayama, K., Ishida, N. and Nakayama, K. I. (2005). Role of serine 10 phosphorylation in p27 stabilization revealed by analysis of p27 knock-in mice harboring a serine 10 mutation. *J. Biol. Chem.* **280**, 1095-1102.
Lee, J. D. and Anderson, K. V. (2008). Morphogenesis of the node and notochord: the cellular basis for the establishment and maintenance of left-right asymmetry in the mouse. *Dev. Dyn.* **237**, 3464-3476.
Levin, M. (2005). Left-right asymmetry in embryonic development: a comprehensive review. *Mech. Dev.* **122**, 3-25.
Lowe, L. A., Supp, D. M., Sampath, K., Yokoyama, T., Wright, C. V., Potter, S. S., Overbeek, P. and Kuehn, M. R. (1996). Conserved left-right asymmetry of nodal expression and alterations in murine situs inversus. *Nature* **381**, 158-161.
Meno, C., Saijoh, Y., Fujii, H., Ikeda, M., Yokoyama, T., Yokoyama, M., Toyoda, Y. and Hamada, H. (1996). Left-right asymmetric expression of the TGF beta-family member lefty in mouse embryos. *Nature* **381**, 151-155.
Meno, C., Shimono, A., Saijoh, Y., Yashiro, K., Mochida, K., Ohishi, S., Noji, S., Kondoh, H. and Hamada, H. (1998). lefty-1 is required for left-right determination as a regulator of lefty-2 and nodal. *Cell* **94**, 287-297.
Mine, N., Anderson, R. M. and Klingensmith, J. (2008). BMP antagonism is required in both the node and lateral plate mesoderm for mammalian left-right axis establishment. *Development* **135**, 2425-2434.
Mishina, Y., Crombie, R., Bradley, A. and Behringer, R. R. (1999). Multiple roles for activin-like kinase-2 signaling during mouse embryogenesis. *Dev. Biol.* **213**, 314-326.
Nonaka, S., Tanaka, Y., Okada, Y., Takeda, S., Harada, A., Kanai, Y., Kido, M. and Hirokawa, N. (1998). Randomization of left-right asymmetry due to loss of nodal cilia generating leftward flow of extraembryonic fluid in mice lacking KIF3B motor protein. *Cell* **95**, 829-837.
Ramsdell, A. F. and Yost, H. J. (1999). Cardiac looping and the vertebrate left-right axis: antagonism of left-sided Vg1 activity by a right-sided ALK2-dependent BMP pathway. *Development* **126**, 5195-5205.
Santos, N. and Reiter, J. F. (2008). Building it up and taking it down: the regulation of vertebrate ciliogenesis. *Dev. Dyn.* **237**, 1972-1981.
Sasaki, H. and Hogan, B. L. (1993). Differential expression of multiple fork head related genes during gastrulation and axial pattern formation in the mouse embryo. *Development* **118**, 47-59.
Soriano, P. (1999). Generalized lacZ expression with the ROSA26 Cre reporter strain. *Nat. Genet.* **21**, 70-71.
Starborg, M., Gell, K., Brundell, E. and Hoog, C. (1996). The murine Ki-67 cell proliferation antigen accumulates in the nucleolar and heterochromatic regions of interphase cells and at the periphery of the mitotic chromosomes in a process essential for cell cycle progression. *J. Cell Sci.* **109**, 143-153.
Sulik, K., Dehart, D. B., Iangaki, T., Carson, J. L., Vrablic, T., Gesteland, K. and Schoenwolf, G. C. (1994). Morphogenesis of the murine node and notochordal plate. *Dev. Dyn.* **201**, 260-278.
Tabin, C. J. (2006). The key to left-right asymmetry. *Cell* **127**, 27-32.
Tallquist, M. D. and Soriano, P. (2000). Epiblast-restricted Cre expression in MORE mice: a tool to distinguish embryonic vs. extra-embryonic gene function. *Genesis* **26**, 113-115.
Tam, P. P. and Behringer, R. R. (1997). Mouse gastrulation: the formation of a mammalian body plan. *Mech. Dev.* **68**, 3-25.
Toyoshima, H. and Hunter, T. (1994). p27, a novel inhibitor of G1 cyclin-Cdk protein kinase activity, is related to p21. *Cell* **78**, 67-74.
Tucker, R. W., Pardee, A. B. and Fujiwara, K. (1979). Centriole ciliation is related to quiescence and DNA synthesis in 3T3 cells. *Cell* **17**, 527-535.
Yokouchi, Y., Vogan, K. J., Pearse, R. V., 2nd and Tabin, C. J. (1999). Antagonistic signaling by Caronte, a novel Cerberus-related gene, establishes left-right asymmetric gene expression. *Cell* **98**, 573-583.
Yoshioka, H., Meno, C., Koshiba, K., Sugihara, M., Itoh, H., Ishimaru, Y., Inoue, T., Ohuchi, H., Semina, E. V., Murray, J. C. et al. (1998). Pitx2, a bicoid-type homeobox gene, is involved in a lefty-signaling pathway in determination of left-right asymmetry. *Cell* **94**, 299-305.